Pergamon

SCIENCE DIRECT®

Bioorganic & Medicinal Chemistry Letters 13 (2003) 69–73

BIOORGANIC & MEDICINAL CHEMISTRY LETTERS

Rational Approaches Towards Reversible Inhibition of Type B Monoamine Oxidase. Design and Evaluation of a Novel 5H-Indeno[1,2-*c*]pyridazin-5-one Derivative

Frédéric Ooms,[a,†] Raphaël Frédérick,[a] François Durant,[a] Jacobus P. Petzer,[b] Neal Castagnoli, Jr.,[b] Cornelis J. Van der Schyf[b,c,‡] and Johan Wouters[a,*]

[a]*Facultés Universitaires Notre-Dame de la Paix, Laboratoire de Chimie Moléculaire Structurale, B-5000 Namur, Belgium*
[b]*Department of Chemistry, The Harvey W. Peters Center, VA-MD Regional College of Veterinary Medicine, Virginia Tech, Blacksburg, VA 24061-0212, USA*
[c]*Department of Biomedical Sciences and Pathobiology, VA-MD Regional College of Veterinary Medicine, Virginia Tech, Blacksburg, VA 24061-0212, USA*

Received 18 June 2002; revised 5 September 2002; accepted 3 October 2002

Abstract—The stereoelectronic properties of several potent reversible monoamine oxidase B (MAO-B) inhibitors were studied with a view to develop a pharmacophore model for reversible MAO-B inhibition. This study suggested that important specific H-bond and hydrophobic interactions are required for potent and selective MAO-B inhibition. These requirements were applied in the design and synthesis of a novel reversible and selective MAO-B inhibitor, 3-methyl-8-(4,4,4-trifluoro-butoxy)indeno[1,2-*c*]pyridazin-5-one, that is ca. 7000 times more selective as an inhibitor for MAO-B than for MAO-A, with $K_{i(MAO\text{-}B)}$ in the low nanomolar range.

Introduction

Monoamine oxidase (MAO; E.C. 1.4.3.4)—an FAD-containing enzyme located in the outer mitochondrial membranes of neuronal, glial and other cells—catalyzes the oxidative deamination of biogenic and xenobiotic amines to the corresponding aldehyde and ammonia in the periphery as well as in the central nervous system.[1] MAO exists in two forms, that is MAO-A and MAO-B: MAO-A preferentially catalyzes the deamination of serotonin, norepinephrine, and epinephrine and is irreversibly inhibited by nanomolar concentrations of the mechanism-based inactivator clorgyline; MAO-B preferentially catalyzes the deamination of β-phenylethyla mine and benzylamine and is irreversibly inhibited by nanomolar concentrations of deprenyl, also a mechanism-based inactivator.[2] Due to the key role played by the two MAO isoforms in the metabolism of neurotransmitters, inhibitors of MAO represent a useful tool for the treatment of several psychiatric and neurological diseases. In particular, reversible and selective MAO-A inhibitors are used as antidepressant and antianxiety drugs, whilst reversible and selective MAO-B inhibitors are under investigation for the treatment of Parkinson's disease (PD) and Alzheimer's disease (AD).[3]

The rational design of reversible MAO-B inhibitors is severely hampered by the lack of a reliable three-dimensional structure of the enzyme catalytic site. We therefore undertook the study of several classes of potent reversible MAO-B inhibitors **1**–**8**[4–10] using an indirect approach to propose a general MAO-B pharmacophore.[11] This study was based on a previously established MAO-B pharmacophore which was obtained from the computation of the molecular electrostatic potential (MEP) generated around representative fragments of the diazoheterocyclic derivatives **1**–**6**.[11]

*Corresponding author. Fax: +32-2526-7270; e-mail: jwouters@fundp.ac.be
†Current address: Euroscreen S.A., Route de Lennik 802, B-1070 Brussels, Belgium.
‡Current address: Department of Pharmaceutical Sciences, Texas Tech University Health Sciences Center, School of Pharmacy, 1300 Coulter, Amarillo, TX 79106, USA.

0960-894X/03/$ - see front matter © 2002 Elsevier Science Ltd. All rights reserved.
PII: S0960-894X(02)00838-7

The development of this MAO-B pharmacophore led to the rational design of 3-methyl-8-(4,4,4-trifluoro-butoxy) indeno[1,2-*c*]pyridazin-5-one (**9**), a very potent and selective reversible MAO-B inhibitor (Table 1). To the best of our knowledge, this compound is among the most potent and selective reversible MAO-B inhibitors yet reported. Finally, with the recent determination of the X-ray crystal structure of human MAO-B,[12] compound **9** was docked within the active site of the enzyme. The results obtained from this docking study support the pharmacophore model established in the drug design work and is the first docking study performed with such a potent and selective reversible MAO-B inhibitor in the crystal structure binding site.

Molecular Modeling Study

Earlier studies suggest that MAO-B inhibitors likely are stabilized within the active site of the enzyme through several hydrogen bonds.[11] Therefore, we used a new computational tool, known as the Molecular Hydrogen-Bonding Potential (MHBP),[13] to identifiy groups that likely would be able to stabilize these compounds (**1**–**8**) inside the active site of the enzyme. This study showed that the MHBPs generated by compounds **1**–**8** (Fig. 1) define a unique pharmacophore pattern complementary to that derived from the study of the MEPs calculated for diazoheterocyclic fragments. For a detailed description of MHBP and its advantages the reader is referred to ref 13.

Calculation of the molecular lipophilic potential (MLP)[14] also showed that compounds **1**–**7** could be stabilized within the MAO-B binding site through hydrophobic interactions between their aryl side chain and amino acid residues residing in the MAO-B active site. This hypothesis agrees with previous studies that also demonstrated a significant role for lipophilic interactions in increasing MAO-B inhibitory activity and selectivity.[4,8,10]

In order to best superimpose compounds **1**–**8** on the pharmacophoric elements just described we performed conformational analyses using high-temperature molecular dynamics (HTMD) with the cff91 forcefield.

All the conformers generated in this way occur within 5 kcal mol^{-1} and were superimposed using a rigid RMS fitting procedure. Although structurally different, the conformations of compounds **1**–**8** could be found among all of the conformers generated by HTMD to optimally align the pharmacophoric elements deduced from the computation of the MLPs and the MHBPs (Fig. 2).

Taking into account all of these data we were able to generate a MAO-B pharmacophore that satisfies the relative three dimensional positions of inhibitor hetero-

Table 1. IC_{50} value measured for MAO-B for compounds **1**–**8** (taken from refs 4–10)[a]

Compd		MAO-B
	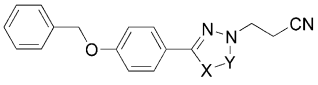	
1	X = O, Y = (C = 0)	2.2
2	X = O, Y = (C = S)	4.4
3	X = S, Y = (C=O)	8.0
4	X = S, Y = (C = S)	16
5	X = (N =), Y = (= N)	2.0
6	X = O, Y = CH2(C=O)	18
7	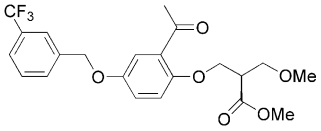	20 nM
8	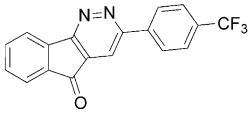	90 nM
9	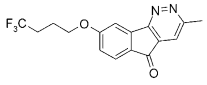	0.014
10	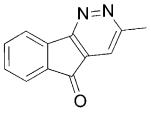	130
11	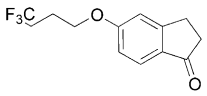	0.318
12	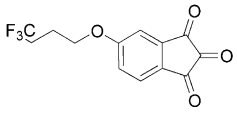	9

[a] K_i values (expressed in μM) for the inhibition of MAO-B by compounds **9**–**12**. For **9**, an approximate K_i value of 100 μM was measured for MAO-A inhibition.

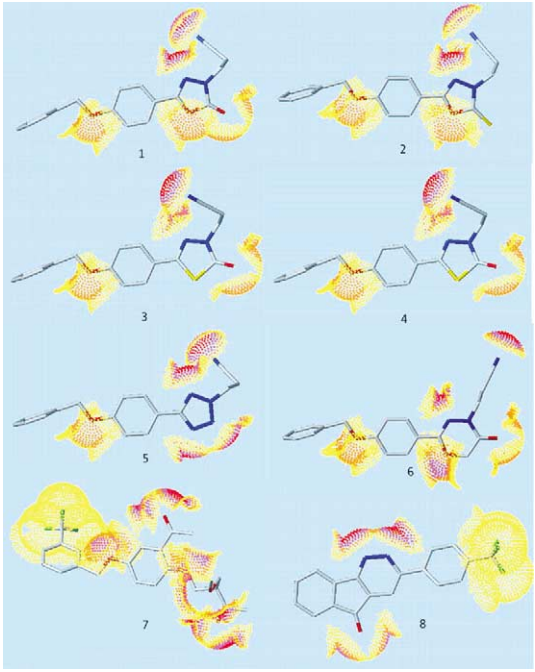

Figure 1. Molecular hydrogen bonding potential (MHBP) calculated on the solvent accessible surface area of compounds **1**–**8**.

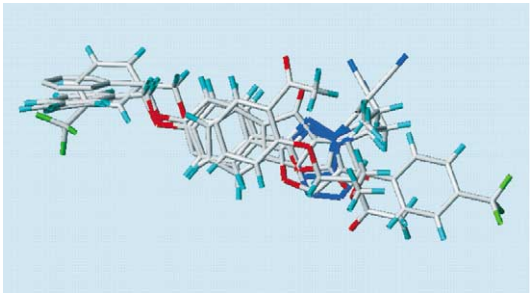

Figure 2. Alignment between compounds **1**–**8** as achieved by RMS fitting between all the pharmacophoric elements.

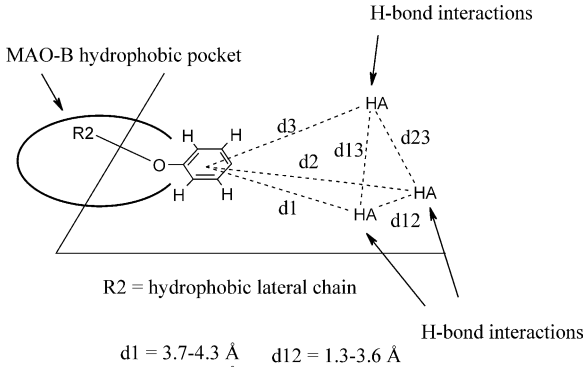

Figure 3. MAO-B pharmacophore model. HA represents the relative position of the hydrogen accepting group.

atoms engaged in H-bonding with amino acid residues within the MAO-B active site (Fig. 3). As deduced from the conformational analyses these heteroatoms are located in the same plane as the aromatic moiety. This model also underscores the crucial role played by the aryl side chain found in compounds **1**–**7**. The aryl side chains in all these compounds are directed towards the same region and it is likely that this structural feature could stabilize these inhibitors through hydrophobic interactions.

According to these results we proposed that substitution of the indeno[1,2-*c*]pyridazin-5-one ring, either on position 7 or 8, should lead to potent and selective MAO-B inhibitors. In order to validate this hypothesis 3-methyl-8-(4,4,4-trifluoro-butoxy)indeno[1,2-*c*]pyridazin-5-one (**9**) was synthesized according to our previously published method (Scheme 1).[15]

MAO Inhibition

Intact mitochondria prepared[16] from human placenta and baboon liver served as sources for MAO-A and MAO-B, respectively. Human placental mitochondria express almost exclusively MAO-A[1] while baboon liver mitochondria express almost exclusively MAO-B.[17] Before use, the mitochondrial homogenate was suspended in sodium phosphate buffer (100 mM, pH 7.4) containing 50% (w/v) glycerol, and the protein concentration (25–60 mg/mL) was determined by the method of Bradford.[18] The inhibition of MAO by the test compounds (**9**–**12**) were evaluated by incubating the nonselective substrate 1-methyl-4-(1-methylpyrrol-2-yl)-1,2,3,6-tetrahydropyridine (MMTP; 30–120 μM) with the mitochondrial homogenate (0.15 mg of protein/mL) and various concentrations of the test compounds. The K_m values of MMTP for MAO-A and MAO-B are 52[19] and 60.9 μM,[17] respectively, in human placental and baboon liver tissue. The test compounds were dissolved in DMSO and added to the buffered incubation mixture such that the final DMSO concentration was 4%. The final volume of the incubation mixtures were 500 μL (in sodium phosphate buffer, pH 7.4) and the samples were incubated at 37 °C for 15 min. The reactions were terminated by the addition of 20 μL perchloric acid (70% v/v), centrifuged (16,000*g* for 5 min) and the concentrations of the enzyme-generated dihydropyridinium metabolite $MMDP^+$ in the supernatant fractions were estimated spectrophotometrically at 420 nm (ε = 25,000 M^{-1} cm^{-1}).[17] These data were used to determine the velocity (V) of the MAO catalyzed oxidation of MMTP.

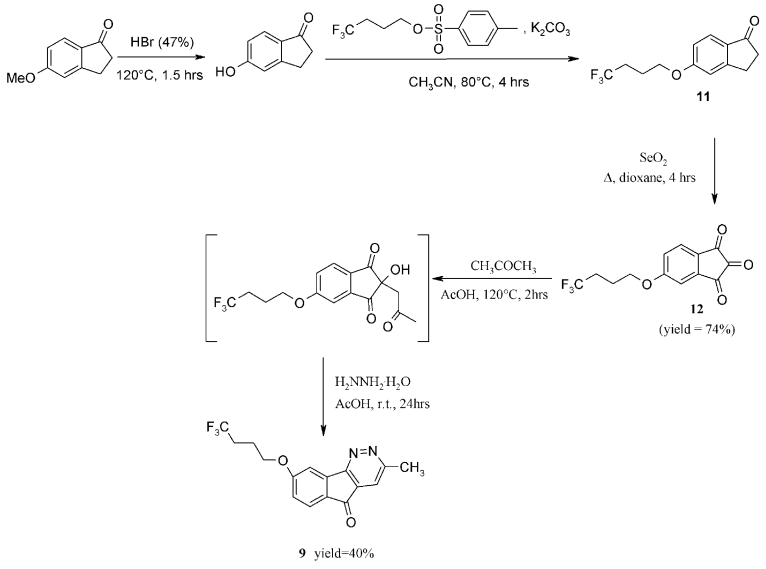

Scheme 1.

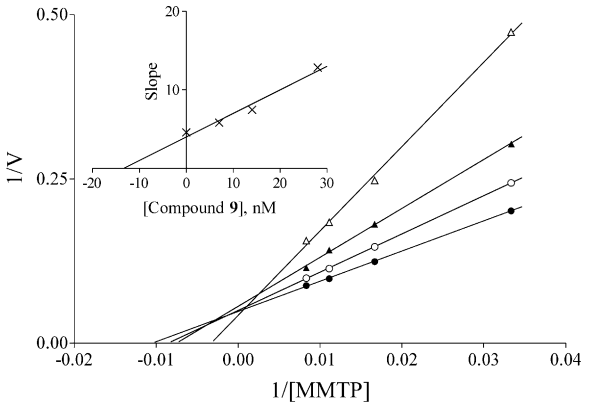

Figure 4. Lineweaver–Burke plots obtained by incubating varying concentrations of the substrate (MMTP) with MAO-B in the absence (filled circles) and presence of different concentrations [7 nM (open circles), 14 nM (filled triangles) and 28 nM (open triangles)] of **9**. The inset is the secondary plot of the slopes versus concentrations of **9**.

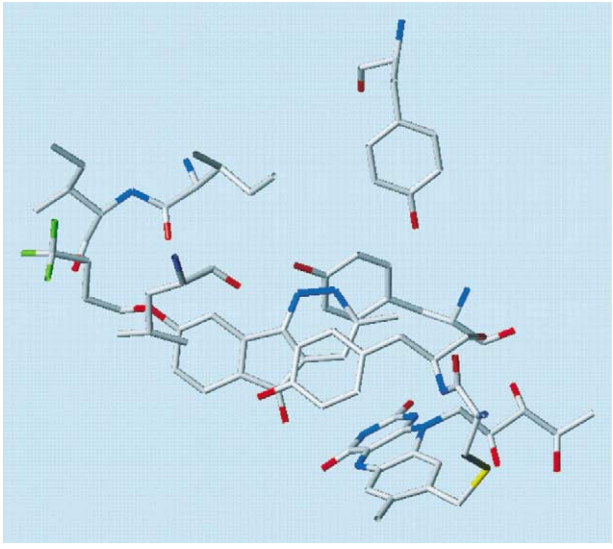

Figure 5. Molecular interaction between compound **9** and amino acid residues of the human MAO-B active site.

Lineweaver–Burke plots with MAO-A and MAO-B were obtained from incubations at four different substrate concentrations with and without three different inhibitor concentrations. The K_i value (x when $y=0$) was determined from a secondary plot in which the values of the slopes obtained from the Lineweaver–Burke plots were plotted as a function of the concentration of the competitive inhibitor.[20] These K_i values are presented in Table 1. The Lineweaver–Burke plots and secondary plot (inset) for **9** are presented in Figure 4. The K_i value for the inbibition of MAO-B by **9** was estimated to be 14 nM (inset, Fig. 4).

Compound **10** and two synthetic intermediates (**11**–**12**) were also tested according to the same experimental protocol (Table 1). These compounds displayed a lower MAO-B inhibitory activity compared to **9** and also satisfied fewer of the requirements for inhibitory activity, suggesting that the pharmacophoric elements determined in this study appear to be essential for MAO-B inhibition.

Docking

Finally, we performed docking of **9** in the active site of the human MAO-B structure obtained through X-ray crystallography (1gos),[12] using the GOLD program.[21] Prior to the docking study the reported crystal structure of human MAO-B was energy minimized after 'removal' of the co-crystallized suicide inhibitor, pargyline. Analysis of the optimal binding mode for **9** (Fig. 5)—identified from the docking study—revealed that compound **9** positions in the vicinity of the FAD cofactor and that the carbonyl and pyridazine functional groups of the indeno[1,2-*c*]pyridazin-5-one nucleus form H-bonds with Tyr-188,-398, and-435. The binding mode adopted by **9** also allows the trifluorobutoxy side chain to settle within a cavity lined with hydrophobic amino acid residues. These data confirm the hypothesis derived from the study of the stereoelectronics of compounds **1**–**8** discussed earlier, and are in accordance with the MAO-B pharmacophore proposed at that time.

Conclusion

Results obtained from studies of the stereoelectronic properties of several putative MAO-B inhibitors afforded coherent information about the nature and spatial location of the main interactions required for reversible MAO-B inhibition, thus guiding the design of novel reversible MAO-B inhibitors. Using these data, we embarked on the rational design of new potent and selective reversible MAO-B inhibitors. Results from this study confirmed that the MAO-B pharmacophore established in this work is a useful tool for the de novo design of potent and selective reversible MAO-B inhibitors with novel structures, exemplified by 3-methyl-8-(4,4,4-trifluoro-butoxy)-indeno[1,2-*c*]pyridazin-5-one (**9**).

Syntheses of other 5*H*-indeno[1,2-*c*]pyridazinones are currently in progress in an attempt to improve the inhibitory potency of **9** even further and to assess the influence on MAOI activity, of varying substitution patterns on the pyridazine ring.

References and Notes

1. Weyler, W.; Hsu, Y. P.; Breakefield, X. O. *Pharmacol. Ther*. **1990**, *47*, 391.
2. Grimsby, J.; Lan, N. C.; Neve, R.; Chen, K.; Shih, J. C. *J. Neurochem*. **1990**, *55*, 1166.
3. Wouters, J. *Curr. Med. Chem*. **1998**, *5*, 137.
4. Lebreton, L.; Curet, O.; Gueddari, S.; Mazouz, F.; Bernard, S.; Burstein, C.; Milcent, R. *J. Med. Chem*. **1995**, *38*, 4786.
5. Mazouz, F.; Gueddari, S.; Burstein, C.; Mansuy, D.; Milcent, R. *J. Med. Chem*. **1993**, *36*, 1157.
6. Mazouz, F.; Lebreton, L.; Milcent, R.; Burstein, C. *Eur. J. Med. Chem*. **1990**, *25*, 659.
7. Mazouz, F.; Lebreton, L.; Milcent, R.; Burstein, C. *Eur. J. Med. Chem*. **1988**, *23*, 441.
8. Kneubühler, S.; Thull, U.; Altomare, C.; Carta, V.; Gaillard, P.; Carrupt, P. A.; Carotti, A.; Testa, B. *J. Med. Chem*. **1995**, *38*, 3874.

9. Kneubühler, S.; Carta, V.; Altomare, C.; Carotti, A.; Testa, B. *Helv. Chim. Acta* **1993**, *76*, 1954.
10. Arvanitis, A. G.; Scholfield, E. L.; Grigoriadis, D.; Heytler, P. G.; Bowdle, J.; Chorvat, R. J. *Bioorg. Med. Chem. Lett.* **1996**, *6*, 115.
11. Wouters, J.; Ooms, F.; Jegham, S.; Koenig, J. J.; George, P.; Durant, F. *Eur. J. Med. Chem.* **1997**, *32*, 721.
12. Binda, C.; Newton-Vinson, P.; Hubalek, F.; Edmondson, D. E.; Mattevi, A. *Nat. Struct. Biol.* **2002**, *9*, 22.
13. Rey, S.; Caron, G.; Ermondi, G.; Gaillard, P.; Pagliara, A.; Carrupt, P. A.; Testa, B. *J. Mol. Graphics Model* **2001**, *19*, 521.
14. Gaillard, P.; Carrupt, P. A.; Testa, B.; Boudon, A. *J. Comput. Aided Mol. Des.* **1994**, *8*, 83.
15. Ooms, F. Rational Approach of the Reversible Inhibition of Type A and B MAO. Design and Synthesis of Original 5H-indeno[1,2-*c*]pyridazin-5-one Derivatives. PhD Thesis, FUNDP, Namur, 2000.
16. Salach, J. I.; Weyler, W. *Methods Enzymol.* **1987**, *142*, 627.
17. Inoue, H.; Castagnoli, K.; Van der Schyf, C.J; Mabic, S.; Igarashi, K.; Castagnoli, N., Jr. *J. Pharmacol. Exp. Ther.* **1999**, *291*, 856.
18. Bradford, M. M. *Anal. Biochem.* **1976**, *72*, 247.
19. Bissel, P.; Bigley, M. C.; Castagnoli, K.; Castagnoli, N., Jr. *Bioorg. Med. Chem.* **2002**, *10*, 3031.
20. Segel, I. H. *Enzyme Kinetics*; Wiley: New York, 1993; p 100.
21. Jones, G.; Willett, P.; Glen, R. C.; Leach, A. R.; Taylor, R. *J. Mol. Biol.* **1997**, *267*, 727.